Available online at www.sciencedirect.com
ScienceDirect
International Journal of Mass Spectrometry 266 (2007) 138–148
International Journal of Mass Spectrometry
www.elsevier.com/locate/ijms

Probing di-nitrobenzene by low energy electrons Identification of isomers via resonances in dissociative electron attachment

Philipp Sulzer [a], Andreas Mauracher [a], Stephan Denifl [a], Michael Probst [a], Tilmann D. Märk [a], Paul Scheier [a], Eugen Illenberger [b,*]

[a] *Institut für Ionenphysik and Angewandte Physik, Center of Molecular Biosciences Innsbruck, Leopold-Franzens-Universität Innsbruck, Technikerstrasse 25, A-6020 Innsbruck, Austria*
[b] *Institut für Chemie und Biochemie-Physikalische und Theoretische Chemie, Freie Universität Berlin, Takustrasse 3, D-14195 Berlin, Germany*

Received 7 June 2007; received in revised form 16 July 2007; accepted 17 July 2007
Available online 2 August 2007

Abstract

Free electron attachment to the three isomers of di-nitrobenzene (DNB) by means of a crossed electron molecular beam experiment with mass spectrometric detection of the anions is studied. In all three isomers, we detect long lived (metastable) non-dissociated parent anions which are formed at energies near 0 eV. In addition, all three compounds exhibit rich fragmentation patterns due to dissociative electron attachment (DEA). The resonance profiles of particular fragment anions in the energy range 0–10 eV differ substantially between the different isomers which can be used for an unambiguous identification of the individual isomer. Many of the DEA products observed at low energy arise from surprisingly complex reactions associated with multiple bond cleavages and structural and electronic rearrangement.

Keywords: Electron attachment; Explosive; Negative ion; Resonance

1. Introduction

DNB belongs to the group of aromatic nitro compounds which have extended use in industrial applications, in particular as explosives or additive to explosives [1]. The most commonly known high explosive is trinitrotoluene (TNT) which has been industrially synthesised since more than 100 years and TNT still serves as a measure for the strength of an explosive. An explosive is characterised by the presence of the elements H, N, C, and O *within* the molecule so that stable compounds like N_2, CO, CO_2 and H_2O can intrinsically be formed. In contrast, the usual combustion of a hydrocarbon only operates by the addition of O_2 so that the velocity of the reaction is limited by diffusion.

Here we explore negative ion formation in the range 0–10 eV to the title compound. It is shown that apart from associative attachment generating a long loved non-dissociated anion, all isomers exhibit rich fragmentation patterns due to DEA. The resonance profiles of particular fragment ions differ substantially when arising from the different isomers which can be used for an unambiguous identification. In conventional mass spectrometry, one detects positive ions following electron impact (mostly at impact energies near 70 eV) and particular compounds may be identified by their specific fragmentation patterns [2]. For different isomers, however, these patterns are usually quite similar which is also the case for the title compounds [3]. Due to the resonant nature of electron capture, the situation can significantly change when recording negative ions [4] as the additional parameter of the electron energy can provide the essential information for isomer identification [5]. Electron impact ionisation (as also photo ionisation) is usually non-resonant in nature (neglecting special features like autoionisation seen in photoionisation mass spectra [6]) and hence the fragmentation patterns and also the ion intensity changes only gradually with the electron energy. A further essential point when comparing cation and anion formation concerns the general cross section behaviour. In electron impact ionisation the total ionisation

* Corresponding author. Tel.: +49 30 838 55350; fax: +49 30 838 56612.
E-mail address: iln@chemie.fu-berlin.de (E. Illenberger).

1387-3806/$ – see front matter © 2007 Elsevier B.V. All rights reserved.
doi:10.1016/j.ijms.2007.07.018

cross section rises gradually above the threshold reaching a maximum at impact energies near 70 eV. At maximum the absolute ionisation cross section may reach values in the order of the geometrical cross section of the molecule [7]. In contrast, the electron capture cross section increases with decreasing electron energy as it follows from very basic physical principles (e.g., Wigner's threshold laws [8]). This means that for molecules possessing appropriate conditions to accommodate an extra electron for some time, the cross section for capturing electrons at very low energy (close to 0 eV) can exceed the geometrical cross section by several orders of magnitude making the production of negative ions at low electron energies most effective [9–11].

Nitrobenzene, nitrotoluene and other aromatic nitrocompounds were studied rather early by using electron beam and swarm techniques [9,12–16]. It was found that these compounds form long-lived molecular anions with lifetimes in the microsecond to millisecond range, in addition they also undergo dissociative electron attachment yielding NO_2^-. Different subsequent studies considered the potential of NO_2^- to serve as a fingerprint for the identification of the neutral compound [17–19] thereby possessing a significant potential as a marker for the detection of explosives [19]. It was recently demonstrated [18] by measuring the NO_2^- resonance energies for a series of nitro aromatic compounds including isomers that it is possible to distinguish between the different compounds. DNT has recently been studied by the combined use of a time-of-flight mass spectrometer and two sector field magnetic mass spectrometer [20]. It is found that the transient negative ion formed upon electron attachment promptly decomposes by the loss of neutral H_2O, N_2O and further fragments. In addition, there is a delayed (metastable) decomposition which in the case of the loss of neutral NO is subjected to an unusual large amount of kinetic energy released to the fragments (1 eV) which underlines the explosive nature of the compound.

Here we present a high resolution DEA study to the three isomers of DNB, namely 1,2-DNB (*ortho*), 1,3-DNB (*meta*) and 1,4-DNB (*para*) in the energy range between 0 and 10 eV. It is shown that at threshold (0 eV) all three isomers form a long-lived metastable anion and a strong DEA signal arising from the loss of a neutral NO molecule. All three isomers can easily be distinguished by the DEA resonance profiles of the various fragments present in the energy range between 0 and 10 eV.

2. Experimental

The experiments were performed in a crossed electron/molecule beams device at the Innsbruck laboratory which has previously been described in detail [21]. In brief, the electron beam is formed in a custom built hemispherical electron monochromator, operated at an energy resolution between 80 and 100 meV (FWHM) and an electron current of ≈20 nA. The three isomers of DNB are solid under normal conditions but with sufficient vapour pressure so that at moderately elevated temperatures an effusive molecular beam can be generated. The beam emanates from a source consisting of a temperature regulated oven and a capillary. Experiments have been performed in the range around 60 °C which is well below the melting temperature. At that temperature one can assume that the molecules are transferred as intact compounds into the gas phase. This is also supported by the fact that the dominant ion observed near 0 eV is the non-dissociated metastable parent anion. Negative ions formed in the crossed beams collision zone are extracted by a weak electric field towards the entrance of the quadrupole mass spectrometer. The mass-selected negative ions are detected by a channeltron using a single pulse counting technique. The intensity of a particular mass-selected negative ion is then recorded as a function of the electron energy.

The electron energy scale is calibrated using the well known SF_6^- signal near 0 eV. The compounds were purchased from Sigma–Aldrich at a stated purity of 99.5% and used as delivered.

3. Results and discussion

3.1. Negative ion mass spectra

Electron attachment to the three isomers of DNB in the range 0–10 eV creates the parent negative ion (M^-) and a series of fragment ions arising from DEA. While the parent negative ion is exclusively formed within a narrow resonance near 0 eV (in all three isomers) the fragment ions appear within characteristic resonant features in the energy range 0–10 eV. Figs. 1 and 2 present the negative ion mass spectra for the three isomers including the fully deuterated compound of *meta*-isomer (1,3-DNB-d4). The

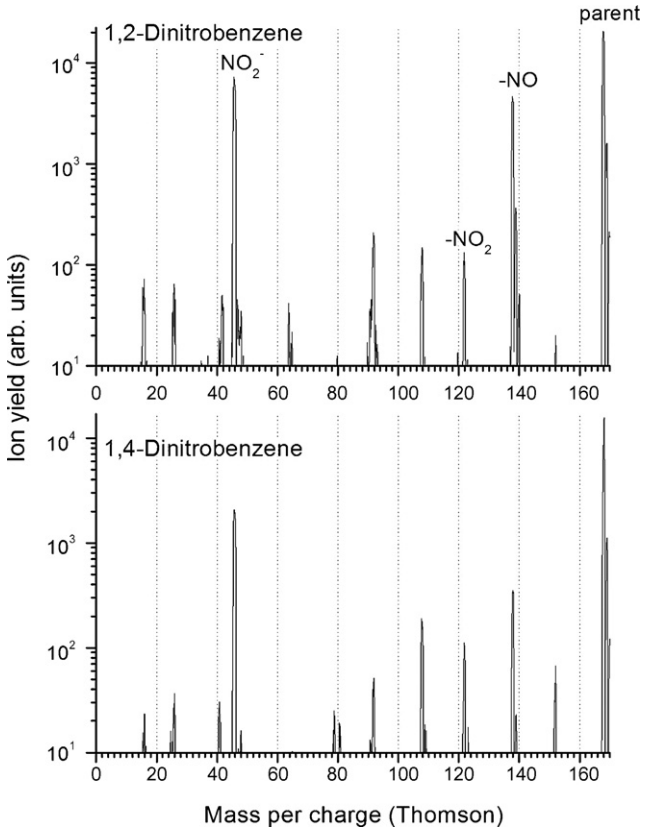

Fig. 1. Negative ion mass spectrum of 1,2-DNB and 1,4 DNB obtained in the electron energy range 0–10 eV in steps of 1 eV by integrating the intensity (see the text).

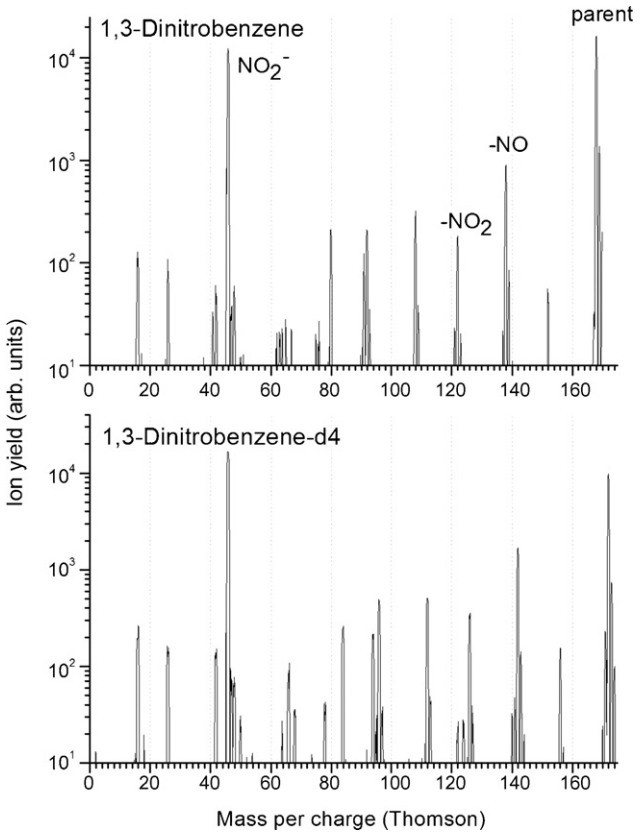

Fig. 2. Negative ion mass spectrum of 1,3-DNB and its fully deuterated analogue, 1,3-DNB-d4 obtained in the electron energy range 0–10 eV in steps of 1 eV by integrating the intensity (see the text).

negative ion mass spectra were obtained by integrating the intensity in the range 0–10 eV via the collection of the ion count rate in steps of 1 eV. All three isomers show common features but also characteristic differences. In the following we shall first assign the main peaks along a line of decreasing mass numbers before considering the explicit ion yield curves of the fragment ions.

168 amu: parent anion $DNB^-/C_6H_4N_2O_4{}^-$, as a dominant signal with some contribution from ^{13}C in its natural abundance seen at 169 and 170 amu (note the logarithmic intensity scale). This signal is shifted by 4 mass units in 1,3-DNB-d4. In 1,3-DNB a small signal is seen at 167 amu is due to the loss of a neutral hydrogen atom via DEA.
138 amu: negative ion formed by the loss of one neutral NO molecule, $(M\text{-}NO)^-/C_6H_4NO_3{}^-$.
122 amu: negative ion formed by the loss of a neutral NO_2 molecule, $(M\text{-}NO_2)^-/C_6H_4NO_2{}^-$.
108 amu: negative ion formed by the loss of two neutral NO molecules, $(M\text{-}2NO)^-/C_6H_4O_2{}^-$.
92 amu: fragment ion formed by the loss of $(NO_2 + NO)$ or N_2O_3, $(M\text{-}N_2O_3)^-/C_6H_4O^-$.

Since the above processes do not involve the loss of H atoms, the corresponding peaks are shifted by 4 mass units in 1,3-DNB-d4.

91 amu: negative ion formed by the loss of neutral (HN_2O_3, $(M\text{-}HN_2O_3)^-/C_6H_3O^-$). Accordingly, in 1,3-DNB-d4 this signal is shifted by only 3 mass units.
46 amu: loss of the fragment ion $NO_2{}^-$ via DEA in all isomers including 1,3-DNB-d4.

On a smaller intensity scale we observe negative ions arising from the loss of neutral O (152 amu) and neutral OH (151 amu) the latter only weakly visible on the spectrum of 1,3-DNB The signal at 42 amu is assigned to NCO^- (a well known pseudohalogen [22]) while that at 41 amu can be assigned as either $CHN_2{}^-$, C_2HO^- or CH_3CN^-. The fact that in 1,3-DNB-d4 only a signal at 42 amu appears excludes CH_3CN^- (the anion of acetonitrile). Both $CHN_2{}^-$ and C_2HO^- are known to exist as stable negative ions [3]. The signal at 25 amu can be assigned to C_2H^- and that at 26 amu to the isobaric fragments $C_2H_2{}^-$ and/or NC^-. Since in 1,3-DNB-d4 only one peak appears at 26 amu we conclude that the peak consists of C_2D^- and possibly CN^-, while formation of $C_2H_2{}^-/C_2D_2{}^-$ (a well known ion having the vinylidene structure C=CH_2 [24]) can be excluded. The ion observed at 80 amu in 1,3-DNB is shifted to 84 amu in 1,3-DNB-d4 which indicates that it carries all four deuterium atoms. A possible assignment of this fragment ion will be given below.

The series of peaks in the mass spectrum of 1,3-DNB around 65 amu (very weak in 1,2-DNB and virtually absent in 1,4-DNB) evolve into three peaks in 1,3-DNB-d4 at 64, 66 and 68 amu. From stoichiometry this can be assigned to the ions N_2C_3 (64 amu) N_2C_3D (66 amu) and $N_2C_3D_2$ (68 amu). The corresponding DEA process (not shown here) peaks at 7 eV where such reactions are certainly accessible.

The mass spectra indicate that the vast majority of fragments formed in the energy range between 0 and 10 eV arise from the loss of neutral and ionic units containing the atoms N, O and H, i.e., fragments preserving the benzene ring structure. Only a few comparatively weak signals (NCO^-, the ion at 80 amu and possibly ions around 65 amu from 1,3-DNB) indicate deterioration of the cyclic structure.

3.2. Electronic structure of the ground state anions

We have calculated the electron affinities of the three isomers by means of the G2(MP2) method [25]. This is an extrapolation method that uses the results from several quantum chemical calculations in order to extrapolate towards molecular energies that would be obtained if complete inclusion of correlations energy and an unlimited basis set were possible. In general, the accuracy of G2(MP2) energies is in the order of about ± 0.2 eV. Hartree-Fock wavefunctions were used to visualize the molecular orbitals and to calculate the dipole moments of the molecules. The program Gaussian 03 [26] was used in all calculations.

Figs. 3 and 4 show the highest occupied molecular orbital (HOMO, MO 43) and the lowest unoccupied molecular orbital (LUMO, MO 44) for neutral 1,3-DNB and 1,4-DNB, respectively. On going to the anionic system MO 44 would correspond to the singly occupied molecular orbital (SOMO) of the molecular anion. The shape of MO 44 is very similar between the neutral and anionic system (the latter not shown here) indi-

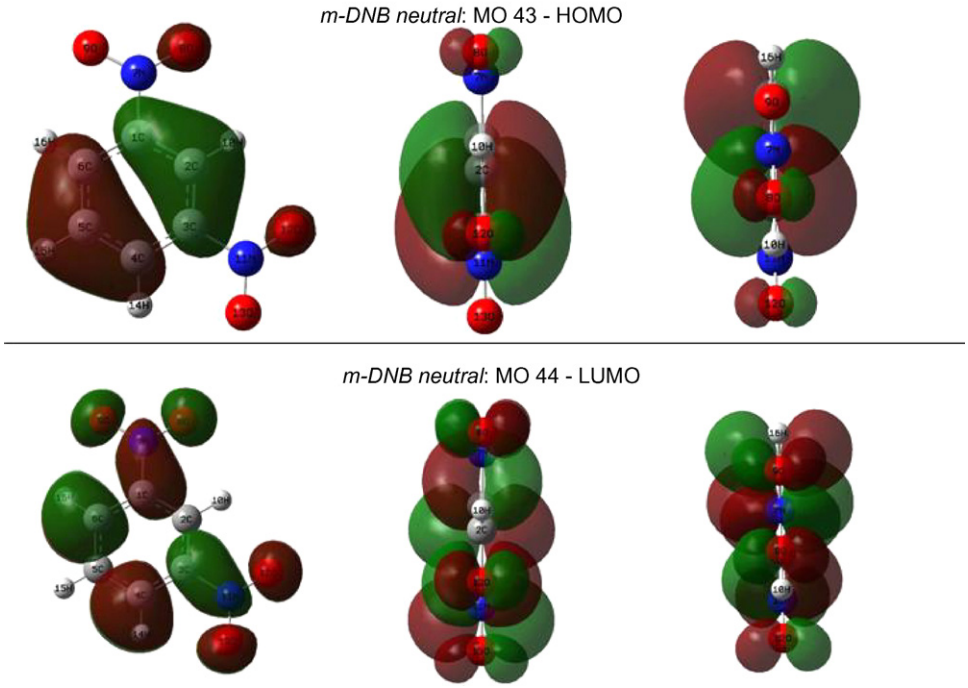

Fig. 3. Graphical representation of MO 43 (HOMO) and MO 44 (LUMO) for neutral 1,3-DNB. By adding an excess charge, MO 44 then represents the singly charged molecular orbital (SOMO) of the anion. Its shape remains virtually unchanged.

cating that it does not change qualitatively. Also, the order of the MOs remains unchanged when adding an excess charge to the system (irrespective whether the anion is calculated at the geometry of the neutral or at its relaxed geometry). From Figs. 3 and 4 it can also be seen that in the anionic ground state the excess electron (MO 44) is delocalised over the ring and the two NO_2 groups. It possesses four nodes along the ring (similar to benzene) and additional nodes between each of the four N–O bonds with some overlap (bonding character) along the C–N bond. It should be mentioned that benzene itself cannot bind an excess electron in a thermodynamically stable state. The lowest anion state of benzene ($^2E_{2u}$) is located at 1.15 eV and can hence directly be accessed by a free electron of that energy [27] which is accommodated into one of the two lowest (degenerate)

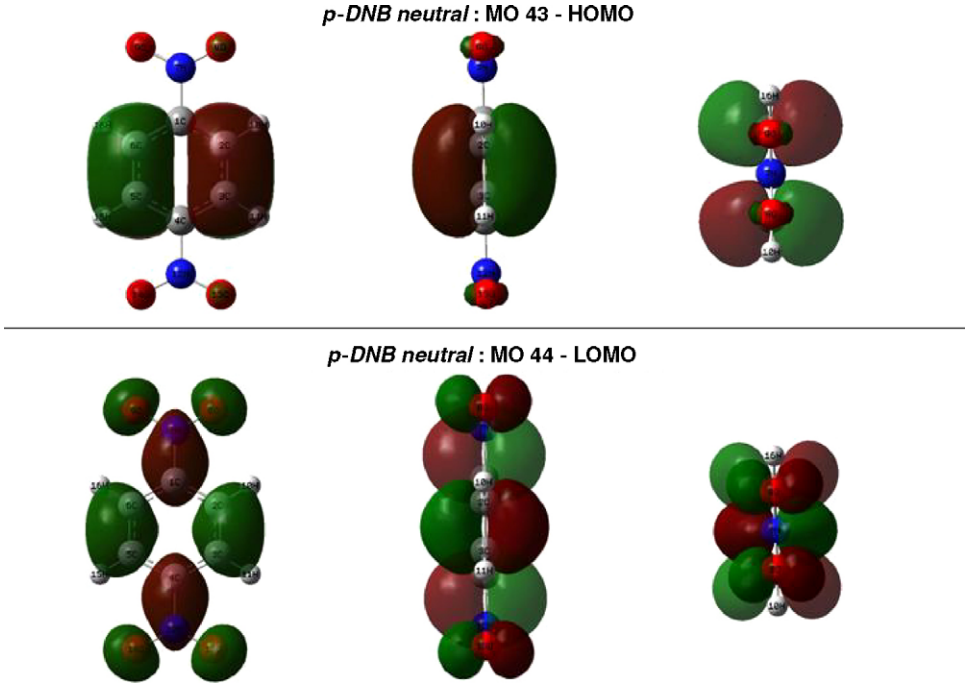

Fig. 4. Graphical representation of MO 43 (HOMO) and MO 44 (LUMO) for neutral 1,4-DNB. By adding an excess charge, MO 44 is transformed into the singly charged molecular orbital (SOMO) of the anion. Its shape remains virtually unchanged.

Table 1
Thermochemical values und electron affinities relevant in dissociative electron attachment to DNB (taken from Ref. [3])

Compound	ΔH_f° (kJ mol^{-1})
1,2-DNT ($C_6H_4N_2O_4$)	-2 ± 0.6 (solid)
1,3-DNT ($C_6H_4N_2O_4$)	−36 (solid)
1,4-DNT ($C_6H_4N_2O_4$)	−38 (solid)
NO_2	33.1
NO	90.29
N_2O_3	82.84
HNO_2 (nitrous acid)	−76.73
CO_2	−393.51

Compound	Electron affinity (eV)
1,2-DNT ($C_6H_4N_2O_4$)	1.65 ± 0.1
1,3-DNT ($C_6H_4N_2O_4$)	1.66 ± 0.1
1,4-DNT ($C_6H_4N_2O_4$)	2.00 ± 0.1
NO_2	2.27
NO	0.026
NCO	3.6090 ± 0.0050
CN	3.8620 ± 0.0050

π^* MOs. By definition benzene possesses a *negative* adiabatic electron affinity (−1.15 eV). In contrast, DNB possesses a positive electron affinity (Table 1). The more extended delocalisation of the excess charge shifts the electron affinity from a negative value in benzene to positive values in all isomers of DNB. Our G2(MP2) *ab initio* calculations predict the following numbers for the adiabatic electron affinities: EA (1,2-DNB) = 1.7 eV, EA (1,3-DNB) = 1.3 eV, and EA (1,4-DNB) = 1.5 eV. The available experimental numbers, obtained from gas phase electron transfer equilibria [3,28], are a few hundred millielectronvolt below the calculated values.

The predicted dipole moments (Hartree-Fock calculations with the 6-311+G(3df,2p) basis set) are 5.0 D (1,2-DNB) and 5.7 D (1,3-DNB). For nitrobenzene, the experimental value is 4.22 D [23]. The dipole moment for 1,3-DNB and 1,4-DNB is hence sufficiently high to allow the binding of an excess electron by the dipolar field (in addition to the valence bound states) [29]. By symmetry, *p*-DNB does not possess a dipole moment, it was, however, shown that an excess electron can weakly be bound (25 meV) by the quadrupolar field of *p*-DNB [30].

3.3. Ion yields and decomposition reactions

In the following we shall consider the explicit ion yields as a function of the energy for the more intense ions as seen in the mass spectra. By just looking at the spectra (Figs. 5–13) one can see that formation of the non-dissociated parent ion is restricted to a narrow feature near 0 eV while all fragment ions show particular resonance profiles indicative of DEA. The spectra shown in Figs. 5–13 are often arbitrarily normalised to the same height for a better visualisation of the different shapes. An estimate of the relative intensities of the different ions can be obtained from the peak heights in the negative ion mass spectra (Figs. 1 and 2).

Before discussing the individual profiles and the underlying reactions we shall briefly recall some essential features concern-

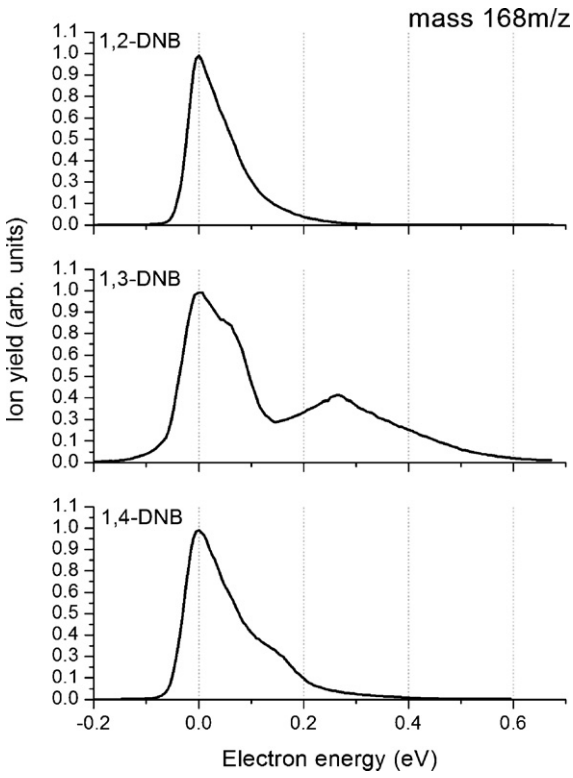

Fig. 5. Yield curve for formation of the non-dissociated parent negative ion in the three isomers of DNB.

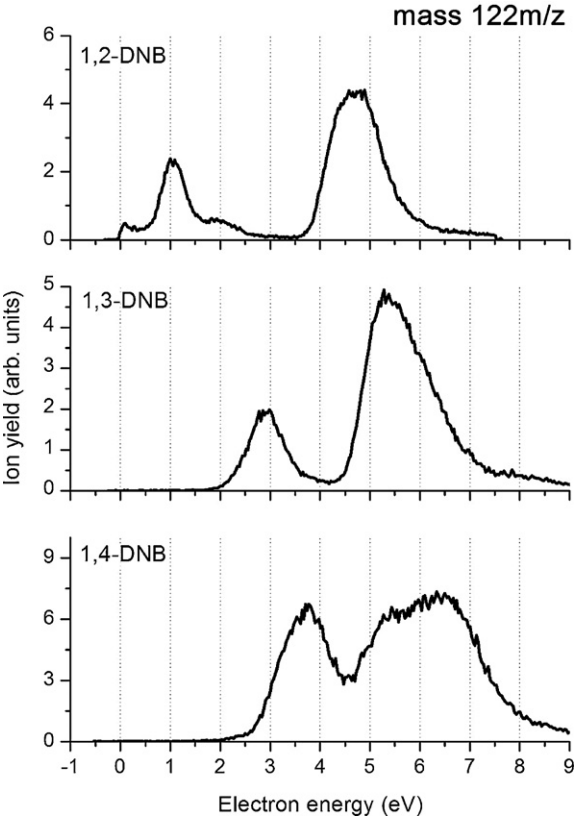

Fig. 6. Relative cross section as a function of the electron energy (ion yield curve) of the ion due to loss of a neutral NO_2 molecule $(M\text{-}NO_2)^-/C_6H_4NO_2^-$ (122 amu).

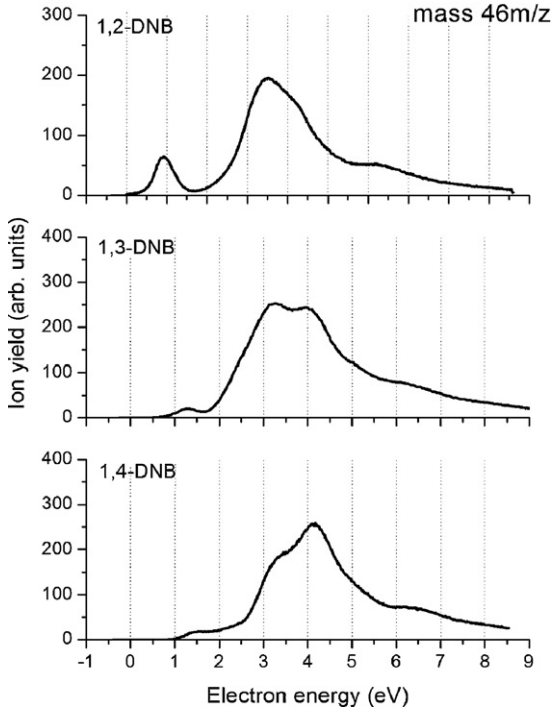

Fig. 7. Ion yield for loss of the ion NO_2^-, representing the complementary fragment ion to $(M\text{-}NO_2)^-/C_6H_4NO_2^-$ (122 amu) with respect to the negative charge (Fig. 6).

ing negative ion formation leading to parent anions (associative electron attachment) and to fragment anions via dissociative electron attachment (DEA).

The capture of a free electron by a polyatomic neutral molecule (symbolised by ABC) generates a transient negative

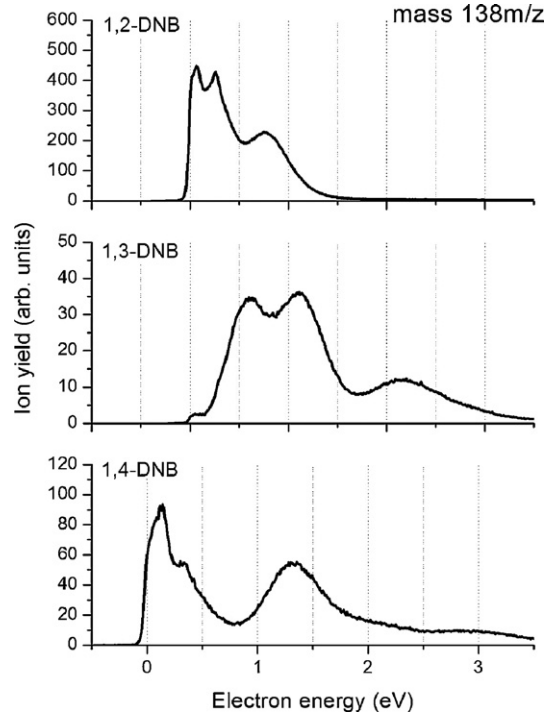

Fig. 8. Yield for the ion due to loss of an NO radical $(M\text{-}NO)^-$ (138 amu).

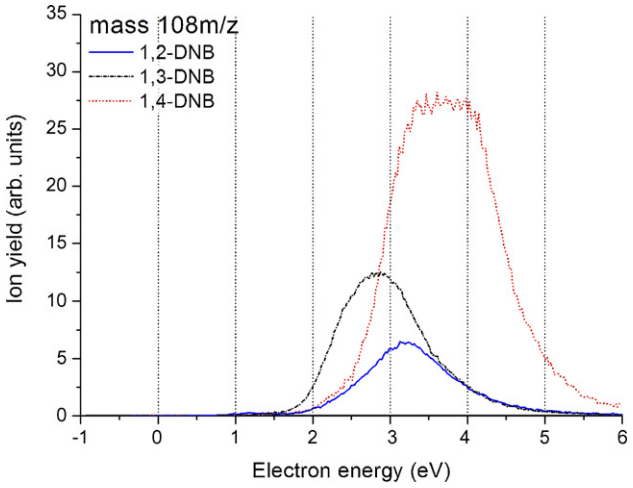

Fig. 9. Yield for the ion due to loss of two NO units $(M\text{-}2NO)^-$ (108 amu).

ion (TNI) or, synonymously, a negative ion resonance (NIR)

$$e^- + ABC \rightarrow ABC^{-\#} \quad (1)$$

Such a compound can be viewed as a quasi-bound state embedded in the autodetachment continuum which is hence intrinsically unstable with respect to the loss of the extra electron. The autodetachment lifetime varies on a large scale dependent on the nature of the target and the electron energy ranging from femtoseconds like in N_2^- [31] to milliseconds like in C_{60}^- [32]. The present molecules thus belong to the group of polyatomic systems where autodetachment is delayed to a degree that the

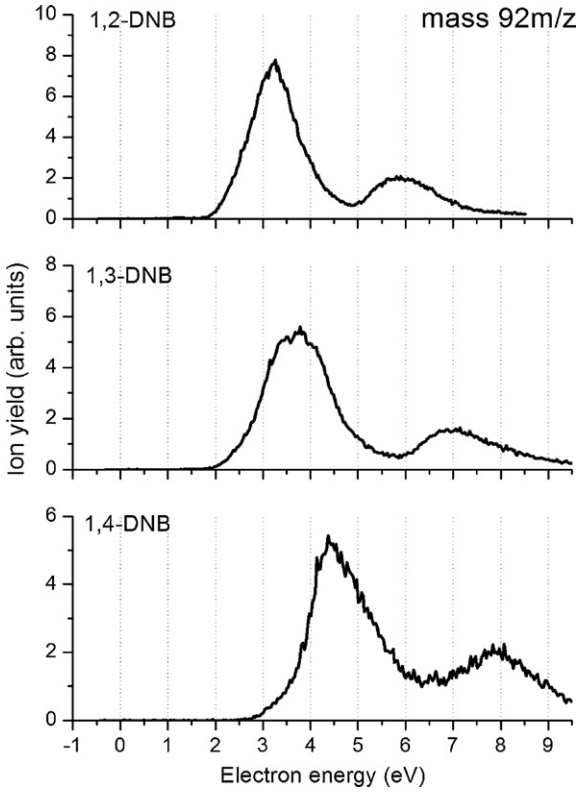

Fig. 10. Yield for the ion due to loss of an NO and NO_2 unit $(M\text{-}N_2O_3)^-$ (92 amu).

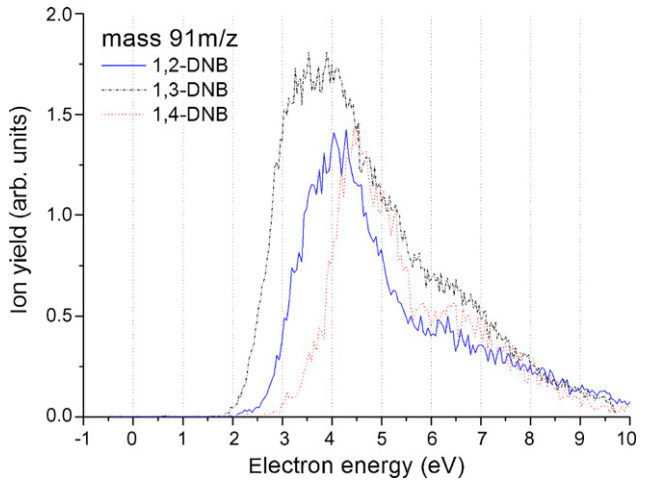

Fig. 11. Yield for the ion due to loss of an NO and HNO_2 unit $(M\text{-}HN_2O_3)^-$ (91 amu).

parent negative ion becomes observable by mass spectrometry. At the same energy (near 0 eV), however, we additionally find one strong DEA channel (loss of neutral NO).

Dependent on the energy of the incoming electron, two types of resonances can be formed, namely single particle *shape* resonances or resonances of the *core excited* type [3,33]. In the first case the excess electron is captured into one of the empty MOs without affecting the configuration of the other electrons while in the second case the incoming electron induces an electronic excitation in the target molecule resulting in two (or more) electrons in normally unoccupied molecular orbitals (MOs). One-particle shape resonances are usually present in the low energy domain (0–≈3 eV) while core excited resonances appear (in addition to shape resonances) at energies in the vicinity of electronic excitation of the neutral molecule.

If dissociation channels are energetically accessible from the transient negative ion, decomposition may take place prior to the loss of the extra electron, *viz.*

$$ABC^{-\#} \rightarrow AB + C^- \qquad (2a)$$

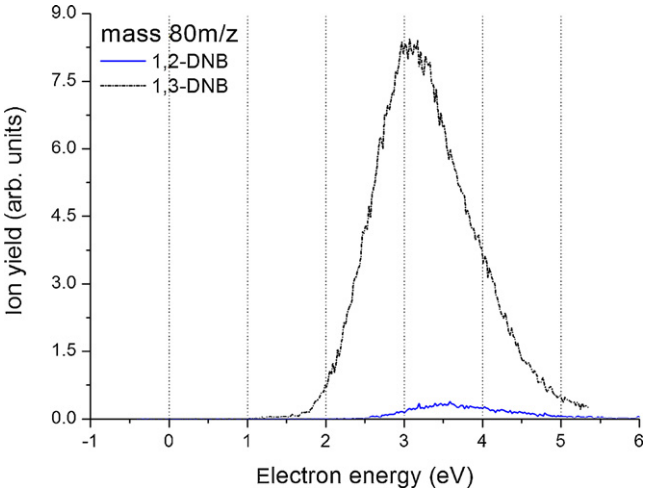

Fig. 12. Yield for the ion $C_5H_4O^-$ (cyclopentadienone) from 1,3-DNB and 1,2-DNB (80 amu).

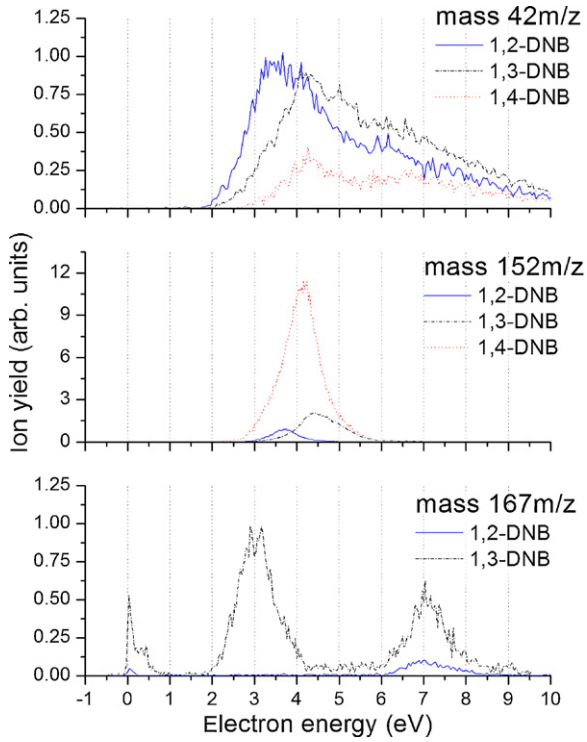

Fig. 13. Ion yield for the fragment at 42 amu (CNO^-), 152 amu (loss of a neutral O) and 167 amu (loss of a neutral H atom).

$$ABC^{-\#} \rightarrow AC + B^- \qquad (2b)$$

Even in the case when the fragment ions (C^-, B^-) appear from the same precursor state located at a particular energy they may carry a gradually different resonance profiles. This is due to the fact that the decomposition into the individual channel (the probability to form a particular fragment ion from the given precursor) has its individual energy dependence which, among others, is also a consequence of autodetachment inherently competing with decomposition.

Energy conservation dictates that the threshold energy (E_{th}) of the DEA reaction (2a) is given by the relation

$$E_{th} = D(AB\text{–}C) - EA(C) \qquad (3a)$$

with D(AB–C) the binding enthalpy of the respective chemical bond and EA(C) the electron affinity of the (neutral) fragment on which the electron becomes localised. In terms of standard heats of formation (ΔH_f°) Eq. (3a) is equivalent to

$$E_{th} = \Delta H_R^\circ = \Delta H_f^\circ(AB) + \Delta H_f^\circ(C^-) - \Delta H_f^\circ(ABC) \qquad (3b)$$

where ΔH_R° assigns the standard reaction enthalpy for process (2a) with $\Delta H_f^\circ(C^-) = \Delta H_f^\circ(C) - EA(C)$.

From the energy balance, fragmentation into more than one neutral fragment is unlikely in the energy range below 4 eV due to the fact that the electron affinity for most radicals is below the strength of a typical chemical bond. This picture, however, is only appropriate for simple bond cleavages. For more complicated reactions involving rearrangement like in (2b), the situation can completely change and multiple fragmentation processes can occur already at very low energies. This is the case,

when rearrangement leads to stable products like the loss of water units from ribose which is observed already near 0 eV [34].

For the interpretation of the experimental results one is hence faced with the two important issues of (i) *the threshold energy of the DEA reaction* under consideration and (ii) *the energy and electronic structure of the transient negative ion* associated with particular DEA reactions. The first quantity can be obtained from established thermochemical data using either the standard heats of formation of the involved species or the appropriate bond dissociation energies and electron affinities. The more difficult quantity is information on the precursor state since it represents a discrete state embedded in the continuum (neutral molecule and an additional electron at infinity). Such *scattering* states cannot be calculated by straightforward variational *ab initio* techniques. Using increasingly larger basis sets will result in an increasingly expanded wave function for the excess electron ultimately leading to the neutral molecule with the excess charge at infinity. A proper treatment of that problem requires the application of scattering calculations [35,36] or particular computational techniques like the stabilisation method [37,38], which artificially keeps the extra charge at the molecule. Such methods, on the other hand, have so far only been applied to shape resonances.

Returning to the ion yields in Figs. 5–13 there is apparently a rich variety of resonant structures in the entire energy range between 0 and 10 eV. Within these structures and the prominent intensity near 0 eV (yielding the non-dissociated parent ion and also the fragment ion due to the loss of NO at 138 amu (Fig. 8)) it appears that most of the fragment ion intensity is concentrated within three main areas, namely in the range around 1 eV, near 4 eV and in the region around 6–7 eV.

For the electronic configuration one can assume that the TNIs at low energy (below 4 eV) can be characterised as shape resonances involving the π^* system while the resonance features at higher energies consist of core excited resonances and possibly also shape resonances.

3.3.1. Parent molecular anion (associative attachment) $M^-/C_6H_4N_2O_4^-$ (168 amu)

Under the present experimental conditions the non-dissociated parent molecular anion is among the dominant signals as already obvious from the mass spectra (Figs. 1 and 2). It is exclusively formed within a comparatively narrow resonance near 0 eV (Fig. 5) with a width only slightly larger than the instrumental energy resolution, however, with a significant tail towards higher energies which is particularly pronounced in 1,3-DNB. The common picture to rationalise the formation of metastable parent anions under collision free conditions is that the electronic energy of the electron attaching system (comprised of the energy of the incoming electron and the electron affinity of the molecule) is effectively dispersed over the vibrational degrees of freedom in the molecule, thereby delaying autodetachment [33]. Along this line we interpret attachment at 0 eV to proceed through the electronic ground state of the anion with the corresponding MOs shown in Figs. 3 and 4.

A prototype system of associative attachment is SF_6 which possesses one of the highest electron attachment cross sections [39]. In SF_6, all DEA channels are endothermic and hence not accessible at 0 eV provided that the temperatures of the target molecule is low (no thermal activation) [40]. In contrast in all three isomers of DNB the parent anion formed at 0 eV additionally undergoes DEA via loss of a neutral NO radical leading to the anion $(M\text{-}NO)^-/C_6H_4NO_3^-$) which significantly contributes to ion formation starting near 0 eV (Fig. 6). It is interesting to note that the ion yield of 1,3-DNB shows a remarkable tail exceeding to about 0.5 eV indicating that this isomer remains metastable towards higher energies. As mentioned above, associative attachment processes leading to mass spectrometrically observable parent ions usually occur within a narrow energy region near 0 eV as also observed for the present systems. A remarkable exception is electron attachment to C_{60} (and other fullerenes) generating metastable parent anions up to electron energies of 10 eV [32]. We again note that very recent experiments on di-nitrotoluene [20] revealed that low energy electron attachment leads to both prompt DEA and a metastable decomposition of the transient anion.

At that point it should also be noted that one has to be extremely careful in interpreting small signals visible right at threshold (0 eV), like those seen on the 167 amu fragment (Fig. 13). Such signals can either be artefacts (Trojan horse ionisation [41]), can arise from small impurities or can be due to hot band transitions [33,42]. Since the DEA cross section behaves reciprocally with the electron energy very small impurities or transitions from vibrationally excited molecules can generate a noticeable signal at 0 eV. Small impurities can also arise from thermal decomposition of the molecule at the hot filament.

In the following we shall consider the dominant DEA processes in light of their difference between the three isomers.

3.3.2. The complementary ions NO_2^- (46 amu) and $(M\text{-}NO_2)^-/C_6H_4NO_2^-$ (122 amu)

These ions arise from the cleavage of one of the two C–N bonds leading to the complementary DEA reactions with respect to the extra charge

$$e^- + DNB \rightarrow (DNB\text{-}NO_2)^- + NO_2 \quad (4a)$$

$$e^- + DNB \rightarrow (DNB\text{-}NO_2) + NO_2^- \quad (4b)$$

Fig. 6 shows the explicit ion yield curve of $(DNB\text{-}NO_2)^-/C_6H_4NO_2^-$ and Fig. 7 that of NO_2^- from the three isomers. The yield curves of the ion $(DNB\text{-}NO_2)^-$ differs remarkably between the isomers in that both the experimental appearance energy and peak position is considerably shifted to higher energy along the line 1,2-DNB, 1,3-DNB and 1,4-DNB. This is a surprising result as from thermodynamics one would not expect any noticeable difference. The thermodynamic threshold for the DEA reactions (4a) and (4b) is given by the C–NO_2 bond dissociation enthalpy minus the electron affinity of that radical, on which the excess charge becomes localised. We have calculated the electron affinities of the different $(M\text{-}NO_2)$ radicals resulting in the following numbers: 2.25 eV (1,2-DNB),

2.10 eV (1,3-DNB), and 2.15 eV (1,4-DNB). Taking the known bond dissociation energy $D(C–NO_2)$ in aromatic nitro compounds (3.1 eV [1]) one arrives at thermodynamic thresholds in the range between about 0.9 and 1.0 eV. The experimental appearance energies and also peak positions, on the other hand, differ by more than 2 eV.

Fig. 6 clearly demonstrates that by recording the fragment ion $(DNB\text{-}NO_2)^-$ the different isomers can easily be distinguished due to their well separated low energy resonances with peak maxima at 1.1 eV (1,2-DNB), 2.7 eV (1,3-DNB), and 3.5 eV (1,4-DNB). This is also an impressive example showing that even in larger polyatomic systems the appearance energy can be located appreciably above the thermodynamic threshold which indicates that the reaction is rather controlled by the electronic structure of the transient ion (via the corresponding Franck–Condon transition) than by thermodynamics. For the low energy resonance associated with $(DNB\text{-}NO_2)^-$ this is most likely a transition generating a shape resonance.

The complementary reaction (4b) also differs between the isomers but less pronounced (Fig. 7). The peak positions of both resonances are also shifted to higher energy along the line 1,2-DNB, 1,3-DNB and 1,4-DNB.

Taking the very well known value for the electron affinity of NO_2 (Table 1) and the $C–NO_2$ binding energy from above (3.1 eV) the thermodynamic limit of (4b) is at about 0.8 eV while the experimental appearance energies are in the range between 0.4 and 1 eV indicating that some thermal activation contributes in the appearance of NO_2^- from 1,2-DNB near the experimental threshold.

In each of the isomers, the signal of NO_2^- is considerably more intense (more than one order of magnitude) than its complement $(DNB\text{-}NO_2)^-$. Since the energetic situation is comparable (similar electron affinities) one would rather expect (from phase space and entropy arguments) that the electron would possess a stronger tendency to get localised on the larger cyclic structure than on NO_2. Such a situation was in fact observed in C_6F_5I [43] on the complementary ions $C_6F_5^-$ and I^-. Both ions are formed within a narrow resonance near 0 eV with $C_6F_5^-$ being more intense by more than one order of magnitude.

3.3.3. $(M\text{-}NO)^-/C_6H_4NO_3^-$ (138 amu)

After NO_2^- this ion is the second intense DEA product, it is formed from all the three isomers right at threshold (Fig. 8). Towards higher energies, the spectra differ substantially between the isomers. For this fragment ion the complementary channel, (formation of NO^-) is not observed, presumably due to the low stability of NO^- with respect to electron detachment. The electron affinity of NO is only 0.026 eV (Table 1) and hence the anion becomes unstable towards autodetachment already at room temperature. We can assume that $(DNB\text{-}NO)^-$ is formed by the loss of the NO molecule and rearrangement to the nitrophenoxyanion, which is presumably an energetically favourable reaction. In nitrobenzene the DEA reaction into NO plus the phenoxyanion is exothermic by more than 1 eV (by taking the established corresponding thermochemical data [3] and the electron affinity of the phenoxyradical (2.25 eV) obtained from photodetachment of the anion [44]. It should be noted that in the present case the deposition of an additional charge with essentially no extra energy triggers a quite complex reaction involving multiple bond cleavage and structural and electronic rearrangement. For each isomer, the fragment ion yield shows a series of energetically overlapping resonances (Fig. 8), indicating that different electronic states of the precursor ion contribute to the present DEA reactions. Near 0 eV NO loss competes with associative attachment generating the non-dissociated anion. In terms of potential energy surfaces this means that the surface accessed by electrons close to 0 eV (most likely the surface of the electronic ground state of the anion) crosses a surface leading to NO loss.

3.3.4. $(M\text{-}2NO)^-/C_6H_4O_2^-$ (108 amu)

This ion appears from the three resonances within broad and nearly unstructured resonances with the maximum shifted to higher energies along the line 1,3-DNB, 1,2-DNB, 1,4-DNB (Fig. 9). Loss of two NO radicals could lead to the formation of a benzoquinone anion for which the two isomers (*para*(1,4) and *ortho*(1,2)benzoquinone) are well known both having an appreciable electron binding energy of 1.86 eV [3]. On the basis of the available thermodynamic data [3] such a reaction is exothermic by about 1.5 eV while the resonance maxima are in the region around 3 eV which may be indicative of a considerable activation energy. Also, as obvious from thermochemistry (Table 1), the neutral products $N_2 + O_2$ are energetically more favourable than 2NO.

3.3.5. $(M\text{-}N_2O_3)^-/C_6H_4O^-$ (92 amu)

This reaction is formally associated with the loss of NO and the loss of NO_2, possibly associated with rearrangement in the neutral channel resulting in N_2O_3 and hence a considerably complex reaction. The position of the first peak is shifted to higher energy along the line 1,2-DNB, 1,3-DNB, 1,4-DNB (Fig. 10), and thus with the distance of the two NO_2 groups. From thermodynamics (Table 1) formation of N_2O_3 is by 41 kJ mol^{-1} more favourable than $NO_2 + NO$. The shift of the second and weaker resonance is along the same line within the isomers and even more pronounced with respect to the peak positions.

3.3.6. $(M\text{-}HN_2O_3)^-/C_6H_3O^-$ (91 amu)

A possible reaction to generate this fragment ion is the loss of NO and HNO_2 (nitrous acid). This reaction is similar to that above, but additionally involving hydrogen transfer. The appearance energy is now shifted along the line 1,3-DNB, 1,2-DNB, 1,4-DNB (Fig. 11) indicating that formation of HNO_2 is most favourable when one C–H bond is located between the neighbouring NO_2 groups.

3.3.7. $C_5H_4O^-$ (80 amu)

From stoichiometry, this ion could be formed by the loss of two CO_2 units which is supported by the observation that the 80 amu peak in the mass spectrum of 1,3-DNB is shifted to 84 amu in the deuterated compound 1,3-DNB-d4 (Fig. 2). On the other hand, a negative ion spectrum obtained from the ^{15}N

labelled 1,3-DNB exhibits a peak at 80 amu and a further spectrum from ^{13}C labelled 1,3-DNB (both spectra not shown here) yields the corresponding peak at 85 amu. Consistent with all these observations would be the loss of (NO_2 + NCO) according to

$$e^- + 1,3\text{-DNB} \rightarrow C_5H_4O^- + NO_2 + NCO \quad (5)$$

with $C_5H_4O^-$ the anion of cyclopentadienone which has previously been observed in electron attachment to benzoquinone [45]. This ion is mainly observed from 1,3-DNB and barely detectable from 1,2-DNB. In 1,4-DNB two small peaks at 79 and 81 amu appear, the first one probably due to the loss of NO_2 + HNCO.

3.4. Fragment ions at low intensity

Fig. 13 finally presents a selection of low intensity fragments. The yield curve of the ion at 42 amu and assigned as CNO^- is shown in Fig. 13 (top). This compound is a well known pseudohalogen having an electron binding energy of 3.61 eV [3]. It is formed by excision of the unit from the target molecule. While the shapes of the ion yield curves are quite similar, the intensity of this ion is particularly low from the *para* compound.

Fig. 13 (middle) shows the yield curves for the ion arising from the loss of an oxygen atom having similar shapes but different peak positions.

In Fig. 13 (bottom), the weak ion yield arising from the loss of one H atom, $(M\text{-}H)^-$, is plotted. Interestingly, this ion is not observed from 1,4-DNB and differs substantially between the remaining isomers as the ion from 1,3-DNB exhibits a pronounced resonance at 3 eV, which is not present on the ion yield from 1,2-DNB. It is not obvious whether the small threshold signals (near 0 eV) are artefacts as mentioned above.

In summary from the results presented here it is obvious, that the three different isomers of di-nitrobenzene can easily be identified via the different resonance profiles observed on a number of different DEA channels. It is thereby evident that electron attachment spectroscopy has a strong potential to detect and identify explosives. The absolute cross section for electron attachment to DNB has so far not been reported and is not directly accessible from the present experiments. For nitrobenzene, a recent beam experiment [46] derives a number of 4.6×10^{-16} cm^2 for DEA into NO_2^- and 3.8×10^{-17} cm^2 for formation of the parent anion. These numbers are comparable to typical absolute electron ionisation cross sections for aromatic compounds at an impact energy of 70 eV. In DNB one expects a larger electron attachment cross section due to the presence of the second NO_2 group.

Acknowledgments

Work supported by the Fonds zur Förderung der wissenschaftlichen Forschung (FWF), Wien, the European Commission, Brussels, via ITS-LEIF and EIPAM and the Deutsche Forschungsgemeinschaft, Bonn.

References

[1] T.B. Brill, K.J. James, Chem. Rev. 93 (1993) 2667.
[2] E. de Hoffmann, V. Stroobant, Mass Spectrometry. Principles and Applications, second ed., John Wiley Sons, Chichester, 2001.
[3] The NIST ChemistryWebbBook, http://webbook.nist.gov/.
[4] E. Illenberger, J. Momigny, Gaseous Molecular Ions. An Introduction to Elementary Processes Induced by Ionization, Steinkopff Verlag/Springer-Verlag, Darmstadt/New York, 1992.
[5] S. Süzer, E. Illenberger, H. Baumgärtel, Org. Mass Spectrom. 19 (1984) 292.
[6] J. Berkowitz, Photoabsorption, Photoionization and Photoelectron Spectroscopy, Academic Press, New York, 1979.
[7] H. Deutsch, K. Becker, S. Matt, T.D. Märk, Int. J. Mass Spectrom. 197 (2000) 37.
[8] E.P. Wigner, Phys. Rev. 73 (1948) 1002.
[9] L.G. Christophorou, D.L. McCorkle, A.A. Christodoulides, in: L.G. Christophorou (Ed.), Electron Attachment Processes in Electron-Molecule Interactions and Their Applications, Academic Press, Orlando, 1984.
[10] D. Klar, M.-W. Ruf, H. Hotop, Aust. J. Phys. 45 (1992) 263.
[11] H. Hotop, M.-W. Ruf, M. Allan, I.I. Fabrikant, Adv. At. Mol. Opt. Phys. 49 (2003) 85.
[12] R.N. Compton, L.G. Christophorou, G.S. Hurst, P.W. Reinhardt, J. Chem. Phys. 45 (1966) 4634.
[13] L.G. Christophorou, R.N. Compton, G.S. Hurst, P.W. Reinhardt, J. Chem. Phys. 45 (1966) 536.
[14] L.G. Christophorou, Atomic and Molecular Radiation Physics, Wiley Interscience, London, 1971.
[15] L.G. Christophorou, A. Hadjiantoniou, J.G. Carter, J. Chem. Soc. Faraday Trans. II 73 (1977) 804.
[16] J.P. Johnson, D.L. McCorkle, L.G. Christophorou, J.G. Carter, J. Chem. Soc. Faraday Trans. II 71 (1975) 1742.
[17] E.C.M. Chen, E.S. Chen, M.S. Milligan, W.E. Wentworth, J.R. Wiley, J. Phys. Chem. 96 (1992) 2385.
[18] C.D. Harvey, M. Eberhart, T. Jones, K.J. Voorhees, J.A. Laramee, R.B. Cody, D.P. Clougherty, J. Phys. Chem. A 110 (2006) 4413.
[19] S. Boumsellek, S.H. Alajajian, A. Chutjian, J. Am. Soc. Mass Spectrom. 3 (1992) 243.
[20] F. Zappa, M. Beikircher, A. Mauracher, S. Denifl, M. Probst, A. Bacher, O. Echt, T.D. Märk, P. Scheier, T.A. Field, K. Graupner, submitted for publication.
[21] D. Muigg, G. Denifl, A. Stamatovic, T.D. Märk, Chem. Phys. 239 (1998) 409.
[22] T. Oster, E. Illenberger, Int. J. Mass Spectrom. Ion Proc. 85 (1988) 125.
[23] D.R. Lide (Ed.), CRC Handbook of Chemistry and Physics, 78th ed., CRC Press, Boca Raton, 1997.
[24] K.M. Ervin, J. Ho, W.C. Lineberger, J. Chem. Phys. 91 (1989) 5974.
[25] L.A. Curtiss, K. Raghavachari, J.A. Pople, J. Chem. Phys. 98 (1993) 1293.
[26] M.J. Frisch, G.W. Trucks, H.B. Schlegel, G.E. Scuseria, M.A. Robb, J.R. Cheeseman, J.A. Montgomery Jr., T. Vreven, K.N. Kudin, J.C. Burant, J.M. Millam, S.S. Iyengar, J. Tomasi, V. Barone, B. Mennucci, M. Cossi, G. Scalmani, N. Rega, G.A. Petersson, H. Nakatsuji, M. Hada, M. Ehara, K. Toyota, R. Fukuda, J. Hasegawa, M. Ishida, T. Nakajima, Y. Honda, O. Kitao, H. Nakai, M. Klene, X. Li, J.E. Knox, H.P. Hratchian, J.B. Cross, V. Bakken, C. Adamo, J. Jaramillo, R. Gomperts, R.E. Stratmann, O. Yazyev, A.J. Austin, R. Cammi, C. Pomelli, J.W. Ochterski, P.Y. Ayala, K. Morokuma, G.A. Voth, P. Salvador, J.J. Dannenberg, V. G. Zakrzewski, S. Dapprich, A.D. Daniels, M.C. Strain, O. Farkas, D.K. Malick, A.D. Rabuck, K. Raghavachari, J.B. Foresman, J.V. Ortiz, Q. Cui, A.G. Baboul, S. Clifford, J. Cioslowski, B.B. Stefanov, G. Liu, A. Liashenko, P. Piskorz, I. Komaromi, R.L. Martin, D.J. Fox, T. Keith, M.A. Al-Laham, C.Y. Peng, A. Nanayakkara, M. Challacombe, P.M.W. Gill, B. Johnson, W. Chen, M.W. Wong, C. Gonzalez, J.A. Pople, Gaussian 03, Revision C.02, Gaussian, Inc., Wallingford, CT, 2004.
[27] M. Allan, J. Electron. Spectrosc. Relat. Phenom. 48 (1989) 219.
[28] S. Chowdhury, E.P. Grimsrud, T. Heinis, P. Kebarle, J. Am. Chem. Soc. 108 (1986) 3630.

[29] H. Abdoul-Carime, C. Desfrancois, Eur. Phys. J. D 2 (1998) 149.
[30] C. Desfrancois, V. Periquet, S.A. Lyapustina, T.P. Lippa, D.W. Robinson, K.H. Bowen, H. Nonaka, R.N. Compton, J. Chem. Phys. 111 (1999) 4569.
[31] G.J. Schulz, Rev. Mod. Phys. 45 (1973) 423.
[32] S. Matejcik, T.D. Märk, P. Spanel, D. Smith, T. Jaffke, E. Illenberger, J. Chem. Phys. 102 (1995) 2516.
[33] E. Illenberger, in: C.-Y. Ng (Ed.), Electron Attachment Processes in Free and Bound Molecules, in Photoionization, Part II. Advanced Series in Physical Chemistry, vol. 10B, Wold Scientific, Singapore, 2000, p. 1063.
[34] I. Bald, J. Kopyra, E. Illenberger, Angew. Chem. Int. Ed. 45 (2006) 4851.
[35] D. Bouchiha, J.D. Gorfinkiel, L.G. Caron, L. Sanche, J. Phys. B: At. Mol. Opt. Phys. 39 (2006) 975.
[36] F.A. Gianturco, R.R. Lucchese, J. Chem. Phys. 120 (2004) 7446.
[37] A.U. Hazi, H.S. Taylor, Phys. Rev. A 1 (1970) 1109.
[38] J. Berdys, I. Anusiewicz, P. Skurski, J. Simons, J. Am. Chem. Soc. 126 (2004) 6441.
[39] D. Klar, M.-W. Ruf, H. Hotop, Int. J. Mass Spectrom. 205 (2001) 93.
[40] Electron attachment to SF6 at room temperature yields a small SF_5^- signal due the slightly endothermic DEA channel $SF_5^- + F$.
[41] H. Drexel, W. Sailer, V. Grill, P. Scheier, E. Illenberger, T.D. Märk, J. Chem. Phys. 118 (2003) 7394.
[42] I. Hahndorf, E. Illenberger, Int. J. Mass Spectrom Ion Proc. 167/168 (1997) 87.
[43] P. Tegeder, L. Lehmann, O. Ingolfsson, E. Illenberger, Zeitschr. Phys. Chem. 195 (1996) 217.
[44] R.F. Gunion, M.K. Gilles, M.L. Pollak, W.C. Lineberger, Int. J. Mass Spectrom. Ion Proc. 117 (1992) 601.
[45] C.D. Cooper, W.T. Naff, R.N. Compton, J. Chem. Phys. 63 (1975) 2752.
[46] A. Pelc, P. Scheier, T.D. Maerk, Vacuum 81 (2007) 1180.